

<sup>12</sup>J. Bardeen, L. N. Cooper, and J. R. Schrieffer, *Phys. Rev.* **108**, 1175 (1957).

<sup>13</sup>D. H. Douglass, Jr. and L. M. Falicov, in *Progress in Low Temperature Physics*, edited by C. J. Gorter

(North-Holland, Amsterdam, 1964), Vol. 4, p. 97.

<sup>14</sup>P. M. Tedrow and R. Meservey, *Phys. Rev. Letters* **27**, 919 (1971).

<sup>15</sup>H. Engler and P. Fulde (unpublished).

PHYSICAL REVIEW B

VOLUME 7, NUMBER 1

1 JANUARY 1973

## Heat Capacity of Vanadium Oxides at Low Temperature

D. B. McWhan, J. P. Remeika, and J. P. Maita

*Bell Laboratories, Murray Hill, New Jersey 07974*

and

H. Okinaka, K. Kosuge, and S. Kachi

*Department of Chemistry, Faculty of Science, Kyoto University, Kyoto, Japan*

(Received 12 July 1972)

The electronic contribution to the heat capacity of  $V_{1.97}O_3$ ,  $V_7O_{13}$ , and  $V_{0.86}W_{0.14}O_2$  is very large, with  $\gamma = (130 \pm 3)$ ,  $(80 \pm 5)$ , and  $(80 \pm 5) \times 10^{-4}$  cal K<sup>-2</sup>/mole V, respectively. Comparison of effective masses calculated from the heat capacity, magnetic susceptibility, and optical properties suggests that the mass enhancement results mainly from spin fluctuations in a strongly correlated electron gas. The magnetic contribution to the entropy of  $V_4O_7$  at 53 K is 0.32 cal K<sup>-1</sup>/mole V.

Many temperature-induced metal-insulator transitions occur in oxides of vanadium<sup>1</sup> and titanium.<sup>2</sup> In  $V_2O_3$  the insulating phase is antiferromagnetic (AF),<sup>1</sup> whereas in  $VO_2$  the insulating phase does not order magnetically down to 1.7 K.<sup>3</sup> In the Magneli phases  $V_nO_{2n-1}$ , where  $3 \leq n \leq 8$ , the metal-insulator transitions and the magnetic ordering occur at different temperatures.<sup>4</sup> The available data are summarized in Fig. 1.<sup>5</sup> It is clear that the properties of the oxides containing (a) two  $d$  electrons per cation ( $V_2O_3$ ), (b) one  $d$  electron per cation ( $VO_2$ ), and (c) a mixture of cations with one or two  $d$  electrons ( $V_nO_{2n-1}$ ) are markedly different. By selecting oxides with specific stoichiometries or appropriate transition-metal impurities, it is possible to obtain samples from each of the different classes which are metallic or insulating at low temperatures. Measurement of the heat capacity of these oxides will provide insight into the nature of the metallic states and also some information about the magnetic contributions to the heat capacity and the driving force behind the metal-insulator transitions. In previous studies it was found that the AF insulating phase of  $V_2O_3$  could be suppressed by the addition of  $Ti_2O_3$ , and a large linear term in the heat capacity was observed in the metallic phase.<sup>6</sup> The AF phase is also suppressed with excess oxygen,<sup>7</sup> and in the present work the heat capacity of metallic  $V_{1.97}O_3$  is compared with that of  $V_2O_3$ .  $V_7O_{13}$  remains metallic down to 2.5 K (see Fig. 1), and its heat capacity is compared with that of  $V_4O_7$ , which is insulating at low temperatures. Finally, the insulating phase of  $VO_2$  can be suppressed by

the addition of  $WO_2$ , and the heat capacity of metallic  $V_{0.86}W_{0.14}O_2$  is compared to that of  $VO_2$ . In all cases the metallic phases are found to have greatly enhanced electronic contributions to the heat capacity. Possible origins of this enhancement and their relationship to the metal-insulator transitions are discussed. The magnetic entropy of  $V_4O_7$  is related to the crystal structure of the insulating phase.

### I. SAMPLE PREPARATION

#### $V_{1.97}O_3$

A single crystal was grown by the vapor-transport method using  $TeCl_4$ <sup>8</sup> and a powder sample of  $V_{1.97}O_3$ . The powder sample was made by heating the appropriate mixture of  $V_2O_3$  and  $V_2O_5$  in an evacuated quartz tube at 600 °C for three days and then at 1000 °C for seven days. A Guinier x-ray powder pattern taken on crushed crystals showed the corundum structure with  $a = 4.948(1)$  Å and  $c = 13.989(2)$  Å. X-ray measurements were made relative to a Si internal standard at 4.2 K using a Philips diffractometer and an Air Products Cryotip attachment. The lattice parameters at 4.2 K are  $a = 4.932(1)$  Å and  $c = 14.002(3)$  Å. As in previous studies on pure and doped metallic  $V_2O_3$ , the  $c$  axis contracts on warming.<sup>9</sup> This probably reflects an expansion of the V-V interatomic distance with decreasing  $c/a$  ratio as in the case of Cr-doped  $V_2O_3$ .<sup>10</sup> The electrical resistivity was found to decrease smoothly with decreasing temperature with  $\rho_{298} \sim 2 \times 10^{-3}$  Ω cm and  $\rho_{298}/\rho_{4.2} \sim 3$ . No anomalous rise in re-

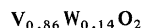
sistivity was observed at low temperatures in the measurements on single crystals as opposed to sintered ceramic samples.<sup>7</sup>



A pressed powder sample was made. The appropriate mixture of  $V_2O_3$  and  $VO_2$  was ground and pressed into a pellet, and this was heated in an evacuated quartz tube at  $800^\circ\text{C}$  for 16 h and then at  $1000^\circ\text{C}$  for 5 h. A Guinier pattern showed only the diffraction lines of  $V_4O_7$ .<sup>11,12</sup> X-ray studies as a function of temperature showed a first-order transition with no change in symmetry at the metal-insulator transition (250 K) and showed no detectable change at the Néel temperature (40 K).<sup>11</sup>



The powder sample was prepared by the usual ceramic techniques. The appropriate mixture of  $V_2O_3$  and  $V_2O_5$  was heated in an evacuated quartz tube at  $600^\circ\text{C}$  for three days and then at  $1000^\circ\text{C}$  for seven days. A Guinier pattern showed the sample to be single-phase  $V_7O_{13}$  in agreement with the data of Andersson and Jahnberg.<sup>12</sup>



The powder sample was prepared from mixtures of  $WO_2$ ,  $V_2O_3$ , and  $V_2O_5$  by the same techniques used for preparing  $V_7O_{13}$ . X-ray studies at room temperature and 4.2 K showed an undistorted rutile structure with  $a = 4.583(2)$  Å and  $c = 2.892(1)$  Å at 298 K and  $a_{298}/a_{4.2} = 1.00076$  and  $c_{298}/c_{4.2} = 1.00483$ .

## II. HEAT-CAPACITY MEASUREMENTS

The heat capacity was measured by the pulsed method of Morin and Maita.<sup>13</sup> The heater and thermometer were attached directly to a crystal of  $V_{1.97}O_3$  which weighed 0.16 g and to the pressed powder cylinder of  $V_4O_7$  which weighed ~1 g. Despite the small noncylindrical shape of the crystal of  $V_{1.97}O_3$  and the porous nature of the pellet of  $V_4O_7$ , the thermometer followed the heat pulses with relaxation times of the order of  $\frac{1}{2}$  sec.

In contrast to  $V_4O_7$  only small quantities of loose powder samples of  $V_7O_{13}$  and  $V_{0.86}W_{0.14}O_2$  were available. In order to make good thermal contact, a mixture of sample-plus-copper powder was pressed in a pellet die to 18 kbar to give a cylindrical sample. Small amounts of pure-copper powder were added to the top and bottom of the mixture to give a smooth surface on which to attach the heater and thermometer. The Cu powder was reduced in hydrogen at  $300^\circ\text{C}$  before use and had a particle size  $< 44 \mu$ . In the experiment on  $V_7O_{13}$ , 0.16 g of sample were mixed with 0.52 g of Cu, and in the experiment on  $V_{0.86}W_{0.14}O_2$  the amounts were 0.23 g of sample and 0.34 g of Cu. The Cu flows around the harder oxide particles and is probably strained.

It is well known that the heat capacity of Cu is increased both by cold working<sup>14</sup> and by annealing in hydrogen.<sup>15</sup> In order to correct for these effects, a pellet of pure Cu was made in the same way as the samples and its heat capacity measured from 1.5 to 25 K. The results were compared with those obtained over the same range on an annealed bulk Cu control sample. It was found that the excess heat capacity of the pellet was given within experimental error by  $\Delta C = 0.16T^2 \times 10^{-4}$  cal  $\text{K}^{-1}/\text{mole Cu}$ . The heat capacity of  $V_7O_{13}$  and  $V_{0.86}W_{0.14}O_2$  was obtained by subtracting the scaled measured heat capacity of the copper pellet from the measured heat capacity of the pellet of sample plus copper. The error resulting from a combination of the nominal 1% accuracy of the measurements on both the sample and the copper pellets varies from 2% at 2.5 K to 6% at 25 K for  $V_7O_{13}$ , where the ratio of sample to Cu in the pellet was the least favorable.

The results are shown in Figs. 2 and 3 for temperatures up to 25 K. For comparison the heat capacity of  $V_2O_3$  and  $VO_2$  is included in Figs. 2 and 3, respectively. The heat capacity may be fitted to the usual linear and cubic terms. There are anomalies in the heat capacity of  $V_{1.97}O_3$ ,  $V_7O_{13}$ , and  $V_{0.86}W_{0.14}O_2$  at low temperatures, and the ex-

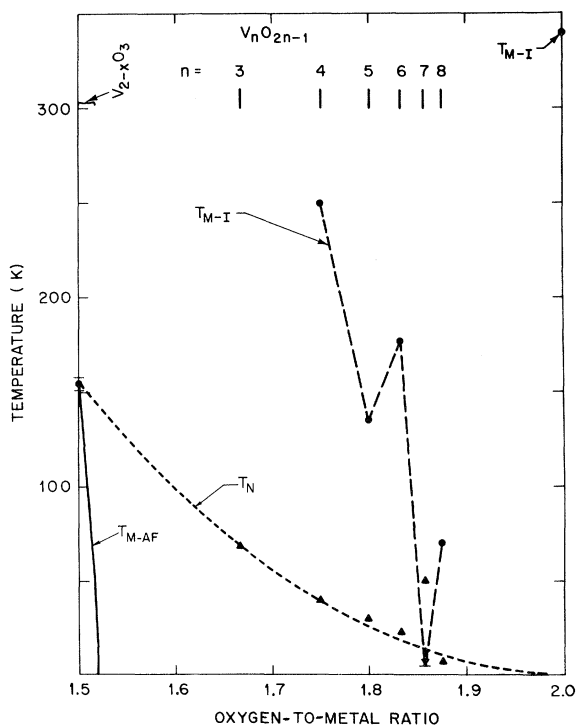


FIG. 1. Comparison of metal-insulator transition temperatures and Néel temperatures for the vanadium oxides. The dotted line is calculated from  $T_N(n) = 155n^{-2}$ . Metallic phases occur at low temperatures in  $V_7O_{13}$  and  $V_{2-x}O_3$ , with  $x > 0.03$  (i. e., oxygen-to-metal ratio  $> 1.53$ ).

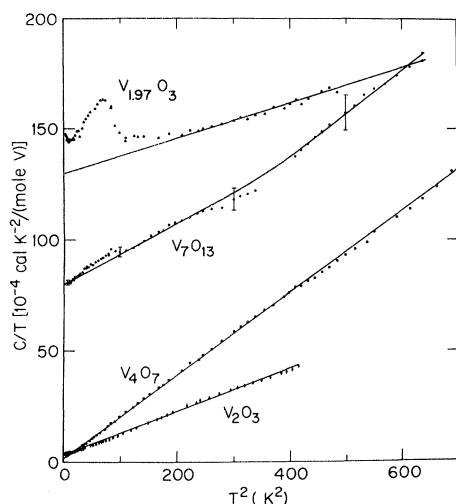


FIG. 2. Heat capacity of several vanadium oxides plotted as  $C/T$  vs  $T^2$  to show the large linear term in the metallic phases. The errors in the data for  $V_4O_7$  and  $V_{1.97}O_3$  are 1%, but the error in the  $V_7O_{13}$  data is indicated by bars. The  $V_2O_3$  data are from Ref. 6.

cess heat capacity over the calculated heat capacity of  $\gamma T + \beta T^3$  is plotted in Fig. 4. These peaks all appear at about the same temperature, which leads one to suspect that they represent a transition in an impurity phase and that they are not intrinsic properties of the materials. No evidence for a transition was observed in either the resistivity or x-ray studies on  $V_{1.97}O_3$ . Finally, these samples were all made from the same starting material, whereas no transition was observed in sam-

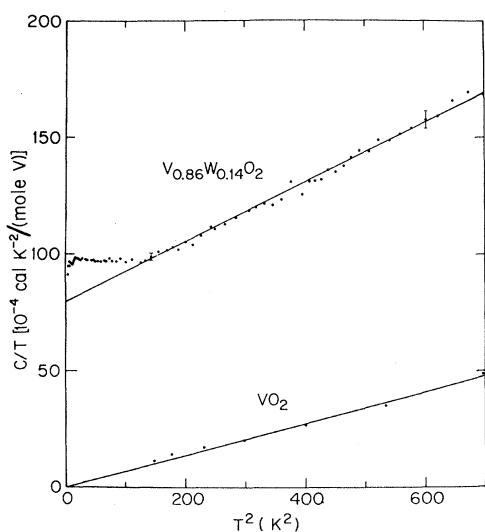


FIG. 3. Comparison of the heat capacity of metallic  $V_{0.86}W_{0.14}O_2$  with that of insulating  $VO_2$ . The latter data are from E. J. Ryder, F. S. L. Hsu, H. J. Guggenheim, and J. E. Kunzler (unpublished).

ples of  $V_4O_7$  and  $(V_{1-x}Ti_x)_2O_3$  which were made from different starting materials.

$V_2O_3$  and  $V_4O_7$  are insulators at low temperatures and the apparent nonzero linear term probably results from a small amount (2–3%) of a second metallic phase. A few percent of a second phase would not be detected in the x-ray powder patterns and is probably not outside the present control over the stoichiometry during sample preparation. Recent experiments on pure  $V_2O_3$  in the insulating phase give  $\gamma = 0$ .<sup>16</sup> Neither the anomalies nor the apparent linear terms will affect the conclusions that will be made about the oxides in Sec. III.

The results for  $V_4O_7$  and  $V_7O_{13}$  up through their respective Néel temperatures are shown in Fig. 5. The observed peak in the heat capacity of  $V_4O_7$  occurs at a lower temperature than the reported Néel temperature of 40 K, but this may reflect differences in stoichiometry. The curve of  $V_7O_{13}$  has been put on the same scale by arbitrarily subtracting a constant linear contribution to the heat capacity. For comparison the heat capacity of  $VO_2$  is included. The lattice contribution to the heat capacity of  $V_4O_7$  can be approximated by that of  $VO_2$  if they are compared for similar numbers of atoms or degrees of freedom. Consequently the points for  $VO_2$  are  $\frac{1}{12}$  times the molar heat capacity of  $VO_2$ . The measurements on  $V_7O_{13}$  at high temperature are only qualitative because of the large contribution from the Cu. The variation with temperature is reliable, but the absolute values at 50 K are only good to 10–15%.

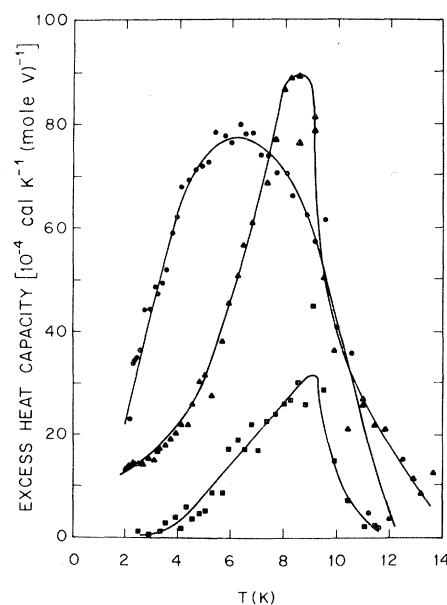


FIG. 4. Excess heat capacity above that calculated from  $\gamma T + \beta T^3$ . Solid triangles,  $0.4\Delta C$  for  $V_{1.97}O_3$ ; solid circles, for  $V_{0.86}W_{0.14}O_2$ ; solid squares, for  $V_7O_{13}$ .

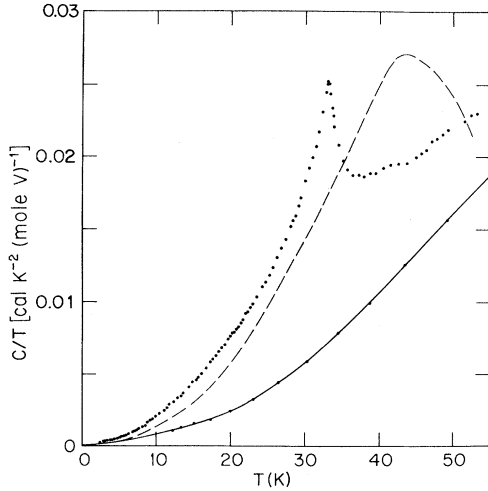


FIG. 5. Heat capacity up through the Néel temperatures of  $V_4O_7$  (closed circles) and  $V_7O_{13}$  (dashed curve). The magnetic contribution to the heat capacity is approximately the difference between  $C/T$  for  $V_4O_7$  and an estimated lattice contribution from  $VO_2$  (solid curve with points). The calculated magnetic entropy up to 53 K is  $0.32 \text{ cal K}^{-1}/\text{mole V}$  in  $V_4O_7$ . The dashed curve for  $V_7O_{13}$  is minus a constant linear term of  $80 \times 10^{-4} \text{ cal K}^{-2}/\text{mole V}$ . Because of the large correction for Cu, the dashed curve is only indicative of the general trend.

### III. DISCUSSION

The heat-capacity data at low temperature can be separated into contributions which vary as  $C_p = \gamma T + \beta T^3$  as shown in Figs. 2 and 3, and the parameters are compared in Table I. The metallic phases all have very large linear terms  $\gamma$ , whereas the insulating phases do not. These values of  $\gamma$  are substantially larger than those found in transition metals or  $4d$  and  $5d$  transition-metal oxides where  $\gamma = 1.7$  (Cu), 23 (Pd), 14 ( $RuO_2$ ), and 13 ( $IrO_2$ ) ( $\times 10^{-4} \text{ cal}^{-2} \text{ K}^{-2}/\text{mole}$ ).<sup>17,18</sup>

Values approaching those in the metallic vanadium oxides are found in high-temperature superconductors such as  $V_3Si$  ( $\gamma = 50 \times 10^{-4} \text{ cal K}^{-2}/\text{mole V}$ ),<sup>19</sup> the itinerant ferromagnet  $ZrZn_2$  ( $\gamma = 90 \times 10^{-4} \text{ cal K}^{-2}/\text{mole Zr}$ ),<sup>20</sup> and cerium intermetallic compounds where the  $f$  levels are believed to be near to the Fermi energy ( $\gamma \sim 100\text{--}500 \times 10^{-4}$ ).<sup>21</sup>

The thermal effective masses compared to those calculated on the basis of a free-electron model are given by  $m_{th}/m_0 = \gamma/\gamma_0$ , where  $\gamma_0 = 2.3 \times 10^{11} N \times (N/V)^{-2/3} \text{ cal K}^{-2}/\text{mole}$ , where  $N$  is the number of  $d$  electrons and  $V$  the volume per mole. The resulting values are  $m_{th}/m = 52$ , 35, and 36 for  $V_{1.974}O_3$ ,  $V_7O_{13}$ , and  $VO_2$ , respectively. Comparable values have been observed in metallic phases of  $V_2O_3$  which were obtained by suppressing the antiferromagnetic insulating phase either by doping with Ti<sup>6</sup> or by the application of pressure<sup>16</sup>;  $m_{th}/m$

= 38 and 31 for  $(V_{0.92}Ti_{0.08})_2O_3$  and for  $V_2O_3$  at  $P = 20$  kbar, respectively.

Large effective masses can result from band-structure effects, strong electron-phonon interactions, or strong electron-electron interactions.<sup>17</sup> In order to choose between these different effects, the thermal effective masses can be compared to those obtained from optical studies and the magnetic susceptibility. The ratio of the number of carriers per  $\text{cm}^3$  to the optical mass,  $N/Vm_{op}$ , is given by the plasma frequency  $\omega_p^2 = 4\pi Ne^2/Vm\epsilon_\infty$ . In  $VO_2$  Barker *et al.* calculate a value  $m_{op}/m = 0.4$  from  $\omega_p = 3.6 \text{ eV}$  and  $n = 30 \times 10^{20} \text{ electrons/cm}^3$ .<sup>22</sup> The value of  $n$  was calculated assuming a one-band model from measurements of the Hall coefficient and the conductivity. Even in a multiband model the number of carriers is not likely to exceed one  $d$  electron per vanadium ( $n = 3.4 \times 10^{22} \text{ cm}^{-3}$ ), and this leads to  $m_{op}/m = 4$ . In both cases the optical mass of metallic  $VO_2$  is about a factor of 10 smaller than the thermal mass obtained for metallic  $V_{0.86}W_{0.14}O_2$ . The optical data for  $V_2O_3$  do not lead to a definitive value for  $\omega_p$ . The optical conductivity shows some structure with increasing frequency which may be due to interband transitions, and it drops between 1 and 3 eV.<sup>23</sup> The optical data are not inconsistent with an optical mass in  $V_2O_3$  of the order of that for  $VO_2$  but it could be higher. If the mass enhancement were due to band-structure effects, then the thermal and optical masses should be similar. The observed difference in the two masses suggests that the enhancement dies out above some characteristic frequency and that it results from a low-energy excitation such as polarons or spin fluctuations.

A theory of spin fluctuations in a highly correlated electron gas near a metal-insulator transition has been proposed by Brinkman and Rice.<sup>24</sup> In this mod-

TABLE I. Coefficients of heat capacity  $C_p = \gamma T + \beta T^3$   $\times 10^{-4} \text{ cal K}^{-1} (\text{mole V})^{-1}$ .

Oxide	$\gamma$	$\beta$
$(V_{0.92}Ti_{0.08})_2O_3$ <sup>a, b</sup>	$96 \pm 3$	$0.163 \pm 8$
$V_2O_3$ <sup>a, b</sup>	$3^c, 0^d$	$0.096 \pm 4$
$V_{1.97}O_3$	$130 \pm 3$	$0.079 \pm 7$
$V_4O_7$	2	$0.187 \pm 3$
$V_7O_{13}$ <sup>b</sup>	$80 \pm 5$	$0.138 \pm 24$
$VO_2$	0	$0.068 \pm 4$
$V_{0.86}W_{0.14}O_2$ <sup>b</sup>	$80 \pm 5$	$0.127 \pm 10$

<sup>a</sup>Reference 6.

<sup>b</sup>Sample in Cu.

<sup>c</sup>Nonzero value may reflect small amount of  $V_{2-x}O_3$  with  $x > 0.025$ .

<sup>d</sup>Reference 16.

el, the number of doubly occupied sites and the discontinuity in the single-particle occupation number at the Fermi surface approach zero with increasing intra-atomic Coulomb repulsion. Consequently, the effective mass appropriate both to the electronic heat capacity  $\gamma$  and to the spin susceptibility  $\chi$  diverges as  $m^*/m = [1 - (U/U_0)^2]^{-1}$ , where  $U_0$  is the critical value for the intra-atomic Coulomb interaction at the metal-insulator transition.<sup>24</sup> The ratio of the density of states calculated from  $\chi$  and  $\gamma$  [ $N(\epsilon_F)$  states/eV molecule =  $1.77 \times 10^3 \gamma$  =  $3.10 \times 10^4 \chi$ , where  $\gamma$  is in cal K<sup>-2</sup>/mole and  $\chi$  in emu/mole] should be close to 1. This is in contrast to paramagnon theory where  $\chi$  is exchange enhanced and  $\gamma$  is mass enhanced so that the ratio of the densities of states,  $\chi/\gamma$ , diverges as the onset of itinerant ferromagnetism is approached.<sup>25</sup> On the other hand, strong electron-phonon interactions lead to an enhancement of the electronic specific heat but, to first approximation, are independent of spin so that  $\chi$  is not enhanced. These simple models suggest that with a large  $\gamma$ ,  $\chi/\gamma \ll 1$  implies strong electron-phonon interactions,  $\chi/\gamma \approx 1$  implies spin fluctuations, and  $\chi/\gamma \gg 1$  implies paramagnons. Although these models are oversimplified and the different effects are not likely to be completely separable, a comparison with experiment may give a qualitative idea of the dominant interactions. In practice, the magnetic susceptibility of most of the vanadium oxides is not temperature independent as expected for simple Pauli paramagnetism. However, between 0 and 300 K the variation is of the order of 20% for V<sub>2</sub>O<sub>3</sub> and VO<sub>2</sub>, so the qualitative conclusions will not be affected. Comparing  $\chi$  and  $\gamma$  in the limit of  $T \rightarrow 0$  K, the value of the ratio for (V<sub>0.92</sub>Ti<sub>0.08</sub>)<sub>2</sub>O<sub>3</sub> is  $\chi/\gamma = 1.8$ .<sup>6</sup> For V<sub>1.97</sub>O<sub>3</sub> both  $\gamma$  and  $\chi$  are 40% larger than for (V<sub>0.92</sub>Ti<sub>0.08</sub>)<sub>2</sub>O<sub>3</sub>, but  $\chi/\gamma = 2.0$ . In VO<sub>2</sub> a ratio of  $\chi/\gamma = 1.3$  is obtained by comparing pure VO<sub>2</sub> ( $\chi_d \sim 0.6 \times 10^{-3}$  emu/mole<sup>26</sup>) and V<sub>0.86</sub>W<sub>0.14</sub>O<sub>2</sub> ( $\gamma = 80 \times 10^{-4}$  cal K<sup>-2</sup>/mole). Thus near V<sub>2</sub>O<sub>3</sub> and VO<sub>2</sub> both  $\chi$  and  $\gamma$  are enhanced by about the same amount as suggested by the spin-fluctuation model. If the electron-phonon interaction were the dominant one, then it is surprising that superconductivity is not observed at low temperatures.

On the other hand, there is substantial evidence that the electron-phonon interaction does play a role in the metallic state in VO<sub>2</sub>. First, the Raman spectra show that the phonon spectrum in the metallic phase is apparently heavily damped.<sup>27</sup> Secondly, the Debye-Waller factors, which reflect the atomic vibrations, are anomalously large (large mean atomic displacements) in the metallic phase of V<sub>0.976</sub>Cr<sub>0.024</sub>O<sub>2</sub> when compared with the insulating phase<sup>28</sup> and neighboring dioxides such as TiO<sub>2</sub><sup>29</sup> and CrO<sub>2</sub>.<sup>30</sup> It appears that a successful model for VO<sub>2</sub> will have to include both electron-

electron and electron-phonon effects.

The phases V<sub>*n*</sub>O<sub>2*n-1*</sub> between V<sub>2</sub>O<sub>3</sub> and VO<sub>2</sub> present a different problem. The electronic heat capacity, as exemplified by metallic V<sub>7</sub>O<sub>13</sub>, is enhanced like V<sub>2</sub>O<sub>3</sub> and VO<sub>2</sub>. On the other hand, the magnetic susceptibility appears to follow a localized model with a Curie-Weiss law  $\chi = C(T - \theta)^{-1} + \chi_0$  with a Curie constant close to that calculated for the appropriate number of localized V<sup>3+</sup>(*d*<sup>2</sup>) and V<sup>4+</sup>(*d*<sup>1</sup>) ions with  $C_{\text{obs}} = 0.53$  and  $C_{\text{calc}} = 0.55$  and with a Weiss temperature close to the observed Néel temperature ( $\theta = -48$  K and  $T_N = 53$  K).<sup>1,4</sup> The value of  $\chi_0$  is also large such that  $\chi_0/\gamma = 1.1$ . There is a strong experimental similarity between V<sub>7</sub>O<sub>13</sub> and some rare-earth intermetallic compounds containing Ce. Their heat capacities are in the range  $\gamma \sim 100-500 \times 10^{-4}$  cal K<sup>-2</sup>/mole and the susceptibilities follow Curie-Weiss relations corresponding to localized Ce<sup>3+</sup>(*f*<sup>1</sup>) ions.<sup>21</sup> These materials are considered in terms of a model with a conduction band crossing a localized 4*f* level. It has been argued that there is no convincing evidence for very narrow *d* bands in vanadium oxides, and that if the conduction was via broad vanadium 4*s* bands, then it is not clear what causes the metal-insulator transitions.<sup>9</sup> On the other hand, in recent nuclear-magnetic-resonance studies of V<sub>4</sub>O<sub>7</sub> and V<sub>7</sub>O<sub>13</sub>, resonances corresponding to distinct V<sup>3+</sup> and V<sup>4+</sup> sites were observed.<sup>31</sup> X-ray-diffraction studies show a slight localization of charge in metallic V<sub>4</sub>O<sub>7</sub> and a rapid increase in localization and metal-metal bonding below the metal-insulator transition.<sup>11</sup> These experiments suggest the presence of localized *d* states on a microsecond time scale. The present heat-capacity data cannot distinguish between this two-band model and a highly correlated single-*d*-band model and further experimental and theoretical studies are needed.

The large electronic contributions to the heat capacity strongly suggest the importance of electron-electron interactions in driving the metal-insulator transition. The electronic entropy in the metallic phase ( $S_{e1} = \gamma T$ ) at the observed transition temperature is remarkably close to the experimental value for the entropy change at the transition. In V<sub>2</sub>O<sub>3</sub> the Clapeyron equation gives  $\Delta S = 1.3$  cal K<sup>-1</sup>/mole V,<sup>6</sup> and values of 1.4<sup>6</sup> and 2.0 are calculated from the heat capacity of (V<sub>0.92</sub>Ti<sub>0.08</sub>)<sub>2</sub>O<sub>3</sub> and V<sub>1.97</sub>O<sub>3</sub>, respectively. In VO<sub>2</sub> the direct measurement of the latent heat of the transition gives  $\Delta S = 3.0$ , whereas using  $\gamma$  for V<sub>0.86</sub>W<sub>0.14</sub>O<sub>2</sub> gives  $S_{e1} = 2.7$  at 340 K. This correlation is quite good, but it does not exclude the possibility that  $\gamma$  will fall off with increasing temperature and that perhaps part of the observed entropy change results from differences in lattice entropy. There is some evidence for this in the (V<sub>1-x</sub>Ti<sub>x</sub>)<sub>2</sub>O<sub>3</sub> system,<sup>6</sup> and the presence of lattice contributions in metallic VO<sub>2</sub> was discussed

above.

Turning to the magnetic ordering found at low temperatures in the phases  $V_nO_{2n-1}$ , it is clear from Fig. 1 that the Néel temperatures of the discrete phases decrease to zero as the average number of  $d$  electrons decreases from two in  $V_2O_3$  to one in  $VO_2$ . In fact, the Néel temperatures of the stoichiometric oxides  $V_nO_{2n-1}$  follow a relation of the form  $T_N(n) = 155n^{-2}$  as illustrated in Fig. 1. The Néel temperature of  $V_7O_{13}$  is above this curve, but it is metallic below  $T_N$ , unlike the other oxides. Introducing disorder as in  $V_{2-x}O_3$  also leads to a departure from this curve and a rapid suppression of the antiferromagnetic state. The x-ray-diffraction studies on insulating  $V_4O_7$  show a structure containing strings of  $V^{3+}$  and  $V^{4+}$  ions running parallel to the pseudorutile  $c$  axis.<sup>11</sup> The  $V^{3+}$  sites and half of the  $V^{4+}$  sites are paired with short metal-metal distances. There are several possible magnetic states for the  $V^{3+}$ - $V^{3+}$  pairs, but if it is assumed that all the pair bonds are nonmagnetic, then there is one  $V^{4+}$  ion left to order magnetically. The magnetic entropy can be estimated by taking the area up to 53 K between the curves for  $V_4O_7$

and the scaled curve for  $VO_2$  in Fig. 5. This entropy of  $\Delta S = 0.32 \text{ cal K}^{-1}$  per vanadium seems fortuitously close to that calculated for one magnetic  $V^{4+}$  out of four vanadium atoms per mole, i. e.,  $\Delta S = \frac{1}{4}R \ln 2 = 0.35 \text{ cal K}^{-1}$ . This model is highly speculative and will have to await more microscopic evidence.

In conclusion, heat-capacity measurements at low temperatures on insulating and metallic vanadium oxides show greatly enhanced thermal effective masses in the metallic phases. Comparison with optical and susceptibility masses and current theories suggests that the enhancement results mainly from spin fluctuations in a strongly correlated electron gas. As suggested previously, the strong electron correlations must play an important role in driving the metal-insulator transition not only in  $V_2O_3$  but also in  $VO_2$ .<sup>32</sup>

#### ACKNOWLEDGMENTS

The authors thank T. M. Rice, W. R. Brinkman, and A. S. Barker, Jr. for many helpful discussions during the course of this work.

<sup>1</sup>K. Kosuge, *J. Phys. Chem. Solids* **28**, 1613 (1967).

<sup>2</sup>R. F. Bartholomew and D. R. Frankl, *Phys. Rev.* **187**, 828 (1969).

<sup>3</sup>A. C. Gossard, D. B. McWhan, and J. P. Remeika, *Phys. Rev. B* **2**, 3762 (1970).

<sup>4</sup>H. Okinaka, K. Kosuge, S. Kachi, M. Takano, and T. Takada, *J. Phys. Soc. Japan* **32**, 1148 (1972).

<sup>5</sup>H. Okinaka, K. Nagasawa, K. Kosuge, Y. Bando, S. Kachi, and T. Takada, *J. Phys. Soc. Japan* **27**, 1366 (1969) ( $V_3O_5$ ); **28**, 798 (1970) ( $V_4O_7$ ); **28**, 803 (1970) ( $V_5O_9$ ); **29**, 245 (1970) ( $V_6O_{11}$ ,  $V_7O_{13}$ ); *Phys. Letters* **33A**, 370 (1970) ( $V_8O_{15}$ ).

<sup>6</sup>D. B. McWhan, J. P. Remeika, T. M. Rice, W. F. Brinkman, J. P. Maita, and A. Menth, *Phys. Rev. Letters* **27**, 941 (1971).

<sup>7</sup>Probably the hexagonal-close-packed array of oxygen atoms remains complete and there are ordered vanadium defects, so that the oxide should be written  $V_{2-x}O_3$ ; D. B. McWhan, A. Menth, and J. P. Remeika, *J. Phys. (Paris)* **32**, C1-1079 (1971).

<sup>8</sup>K. Nagasawa, Y. Bando, and T. Takada, *J. Appl. Phys. (Japan)* **8**, 1262 (1969).

<sup>9</sup>D. B. McWhan, A. Menth, J. P. Remeika, W. F. Brinkman, and T. M. Rice, *Phys. Rev. B* (to be published).

<sup>10</sup>P. D. Dernier, *J. Phys. Chem. Solids* **31**, 2569 (1970).

<sup>11</sup>M. Marezio, D. B. McWhan, P. D. Dernier, and J. P. Remeika, *J. Solid State Chem.* (to be published).

<sup>12</sup>S. Andersson and L. Jahnberg, *Arkiv Kemi* **21**, 413 (1963).

<sup>13</sup>F. J. Morin and J. P. Maita, *Phys. Rev.* **129**, 1115 (1963).

<sup>14</sup>G. Ahlers, *Rev. Sci. Instr.* **37**, 477 (1966).

<sup>15</sup>D. L. Martin, *Rev. Sci. Instr.* **38**, 1738 (1967).

<sup>16</sup>D. B. McWhan, J. P. Remeika, S. Bader, B. B. Triplett, and N. E. Phillips, *Phys. Rev. B* (to be published).

<sup>17</sup>C. Kittel, *Introduction to Solid State Physics*, 4th ed. (Wiley, New York, 1971).

<sup>18</sup>B. C. Passenheim and D. C. McCollum, *J. Chem. Phys.* **51**, 320 (1969).

<sup>19</sup>J. E. Kunzler, J. P. Maita, H. J. Levinstein, and E. J. Ryder, *Phys. Rev.* **143**, 390 (1966).

<sup>20</sup>J. P. Maita, quoted in G. S. Knapp, F. Y. Fradin, and H. V. Culbert, *J. Appl. Phys.* **42**, 1341 (1971).

<sup>21</sup>J. R. Cooper, C. Rizzuto, and G. Olcese, *J. Phys. (Paris)* **32**, C1-1136 (1971).

<sup>22</sup>A. S. Barker, Jr., H. W. Verleur, and H. J. Guggenheim, *Phys. Rev. Letters* **17**, 1286 (1966); H. W. Verleur, A. S. Barker, Jr., and C. N. Berglund, *Phys. Rev.* **172**, 788 (1968).

<sup>23</sup>A. S. Barker, Jr. and J. P. Remeika, *Solid State Commun.* **8**, 1521 (1970).

<sup>24</sup>W. F. Brinkman and T. M. Rice, *Phys. Rev. B* **2**, 4302 (1970).

<sup>25</sup>J. R. Schrieffer, *J. Appl. Phys.* **39**, 642 (1968).

<sup>26</sup>J. P. Pouget, P. Lederer, D. S. Schreiber, H. Lanois, D. Wohlleben, A. Casalot, and G. Villeneuve, *J. Phys. Chem. Solids* **33**, 1961 (1972).

<sup>27</sup>R. Srivastava and L. L. Chase, *Phys. Rev. Letters* **27**, 727 (1971).

<sup>28</sup>M. Marezio, D. B. McWhan, J. P. Remeika, and P. D. Dernier, *Phys. Rev. B* **5**, 2541 (1972).

<sup>29</sup>R. C. Abrahams and J. L. Bernstein, *J. Chem. Phys.* **55**, 3206 (1971).

<sup>30</sup>P. Porta, M. Marezio, J. P. Remeika, and P. D. Dernier, *Mat. Res. Bull.* **7**, 157 (1972).

<sup>31</sup>A. C. Gossard and J. P. Remeika, *Bull. Am. Phys. Soc.* **17**, 359 (1972).

<sup>32</sup>T. M. Rice, D. B. McWhan, and W. F. Brinkman, in *Proceedings of the Tenth International Conference on the Physics of Semiconductors, Cambridge, 1970*, edited

by S. P. Keller, J. C. Hensel, and F. Stein (National Technical Information Service, Springfield, Va., 1970), p. 6293.

## Landau Model for the Critical Susceptibility of a Ferromagnet\*

P. M. Horn, Ronald Bass, and R. D. Parks

*Department of Physics and Astronomy, University of Rochester, Rochester, New York 14627*

(Received 9 August 1972)

Measurements have been made of the low-field magnetic susceptibility of the ferromagnet GdNi<sub>2</sub> in the reduced temperature interval  $10^{-3} < \epsilon = (T - T_c)/T_c < 4$ . The study focuses on the transition from Curie-Weiss behavior for  $T \gg T_c$  to critical behavior for  $T = T_c$ . A phenomenological model based on Landau's theory of second-order phase transitions is presented which fits the experimental data in this interpolation region. The viability of a Landau model for predicting microscopic exchange interactions (from an analysis of the high-temperature susceptibility) is discussed critically.

The success of the high-temperature Ising and Heisenberg expansions has been well documented<sup>1</sup> and has recently been extended to include next-nearest-neighbor interactions.<sup>2,3</sup> However, in the presence of long-range forces, these expansions become cumbersome and present severe convergence problems<sup>4</sup> for  $T$  near  $T_c$ . To deal with the case of long-range forces, we have developed a phenomenological model based on Marčelja's<sup>5</sup> first-order correction to mean-field theory. It will become evident herein that GdNi<sub>2</sub> has an unusually long interspin force range<sup>6</sup> and as such is particularly well suited for a study of this type.

As a starting point we take the phenomenological model of Landau<sup>7,8</sup> which suggests that the free-energy density at a second-order magnetic transition can be expanded in a power series of even powers of the magnetization:

$$F = \int d^3r \mathcal{F}(r) \\ = \int d^3r \{ h_z(r) M_z(r) + a(T) [M_z(r)]^2 \\ + \frac{1}{2} b [M_z(r)]^4 + \dots + c [\nabla M_z(r)]^2 + \dots \}, \quad (1)$$

where  $h_z(r)$  is the applied magnetic field. The term  $\frac{1}{2} b [M_z(r)]^4$  represents<sup>5</sup> the first-order (two-body) interaction between order-parameter excitations. Neglecting this term in  $F$  leads (through standard techniques<sup>9</sup>) to a mean-field form<sup>9</sup> for the susceptibility [i. e.,

$$\chi^{-1} = \chi_{\text{MF}}^{-1} = 2a_0(T - T_c^{\text{MF}})/T_c^{\text{MF}} \equiv 2a_0\epsilon^{\text{MF}},$$

where  $T_c^{\text{MF}}$  is the mean-field transition temperature].

Recent work by Marčelja<sup>5</sup> has suggested a self-consistent technique for inclusion of the first interaction term. Following his ideas within the framework of the Hartree-Fock approximation<sup>10</sup>

yields

$$\frac{1}{2} b [M_z(r)]^4 = 2b \langle M_z^2(r) \rangle M_z^2(r). \quad (2)$$

Keeping only terms explicitly shown in Eq. (1), the Fourier transform of  $F$  in zero magnetic field becomes

$$F = \sum_k \epsilon(k) M_k^2, \quad (3)$$

where

$$\epsilon(k) = a + 2b \langle M_z^2(r) \rangle + ck^2. \quad (4)$$

Using classical statistics, we obtain for the static correlation function

$$\langle |M_k|^2 \rangle = \frac{k_B T / 2c}{[a + 2b \langle M_z^2(r) \rangle] / c + k^2}. \quad (5)$$

Note that in Eq. (5) the correlation function has the Ornstein-Zernike (OZ) form<sup>11</sup> with  $\xi^2(T) = c/[a + 2b \langle M_z^2(r) \rangle]$ . [Note also that

$$\xi^2(T) \xrightarrow{T \gg T_c} \frac{c}{a_0(T - T_c^{\text{MF}})/T_c^{\text{MF}}} \equiv \frac{\xi^2(0)}{\epsilon^{\text{MF}}}$$

as required.] Equations of the OZ form have the difficulty that they are only valid in the long-wavelength (i. e., small- $k$ ) limit. Thus macroscopic averages over all  $k$  values such as

$$\langle M_z^2(r) \rangle \propto \int d^3k \langle |M_k|^2 \rangle \quad (6)$$

are divergent and require *ad hoc* cutoffs of the momentum integrals. This problem arises because the magnetization is strongly dependent on the behavior of  $\epsilon(k)$  for  $k$  large. Thus, the small- $k$  approximation generated by keeping only one gradient term in the free-energy expansion leads to a susceptibility which is dependent on the choice of the upper cutoff for the momentum integrals.